J|A|C|S COMMUNICATIONS

Published on Web 11/24/2010

Graphene Oxide Nanocolloids

Jiayan Luo, Laura J. Cote, Vincent C. Tung, Alvin T. L. Tan, Philip E. Goins, Jinsong Wu, and Jiaxing Huang*

Department of Materials Science and Engineering, Northwestern University, Evanston, Illinois 60208, United States

Received September 2, 2010; E-mail: jiaxing-huang@northwestern.edu

Abstract: Graphene oxide (GO) nanocolloids—sheets with lateral dimension smaller than 100 nm—were synthesized by chemical exfoliation of graphite nanofibers, in which the graphene planes are coin-stacked along the length of the nanofibers. Since the upper size limit is predetermined by the diameter of the nanofiber precursor, the size distribution of the GO nanosheets is much more uniform than that of common GO synthesized from graphite powders. The size can be further tuned by the oxidation time. Compared to the micrometer-sized, regular GO sheets, nano GO has very similar spectroscopic characteristics and chemical properties but very different solution properties, such as surface activity and colloidal stability. Due to higher charge density originating from their higher edge-to-area ratios, aqueous GO nanocolloids are significantly more stable. Dispersions of GO nanocolloids can sustain high-speed centrifugation and remain stable even after chemical reduction, which would result in aggregates for regular GO. Therefore, nano GO can act as a better dispersing agent for insoluble materials (e.g., carbon nanotubes) in water, creating a more stable colloidal dispersion.

Graphene oxide (GO) is typically made by chemical exfoliation of graphite powders using strong oxidants such as $KMnO_4$ dissolved in concentrated H_2SO_4.[1−4] During reaction and processing, the graphene sheets in the particles are not only derivatized with oxygen-containing groups[5,6] but also torn up into smaller pieces. As a result, the lateral sizes of the as-synthesized GO sheets are usually very polydisperse, ranging from a few nanometers to tens of micrometers,[7,8] which may even vary from synthesis to synthesis. Although it has been noted that prolonged oxidation[9] and sonication[10] can break the sheets into smaller sizes, such random, top-down, size reduction approaches are unlikely to result in uniform size distribution. So far, size-controlled synthesis[9] of small GO sheets has not been extensively studied, partially due to the lack of interest and knowledge on their size-dependent properties. Although a tremendous amount of work has been done to explore the size- and shape-dependent electronic properties of graphene nanostructures,[11−14] nano GO and its graphene product have caught much less interest, presumably due to the highly defective nature of GO. Recently we revealed that GO sheets can act as surfactants with size-dependent amphiphilicity.[15] Smaller GO sheets should be more hydrophilic due to the higher density of charges originating from the ionized −COOH groups on their edges, which suggests that the colloidal stability of GO should also be size-dependent. This motivates us to explore direct synthetic methods for making small GO sheets with a more uniform size distribution. On the other hand, GO nanosheets (<100 nm) have recently been used in cellular imaging[16] and drug delivery[17−19] studies, in which the large micrometer-sized GO sheets have to be removed. Although this could be done by extensive size separation steps (e.g., density gradient separation[20,21]) to extract only the nano GO from the polydisperse samples, direct synthesis will be highly desirable, as it eliminates many processing steps that could adversely affect the colloidal stability or introduce impurities to the highly adsorbing GO sheets. Here we report a size-controlled synthesis of GO nanosheets using graphite nanofibers[22,23] as the precursor. Both GO nanosheets and their reduced form are significantly more stable than their counterparts made from graphite powders (hereafter named regular GO). In addition, GO nanosheets can better disperse insoluble materials such as carbon nanotubes, creating a more stable colloidal dispersion in water.

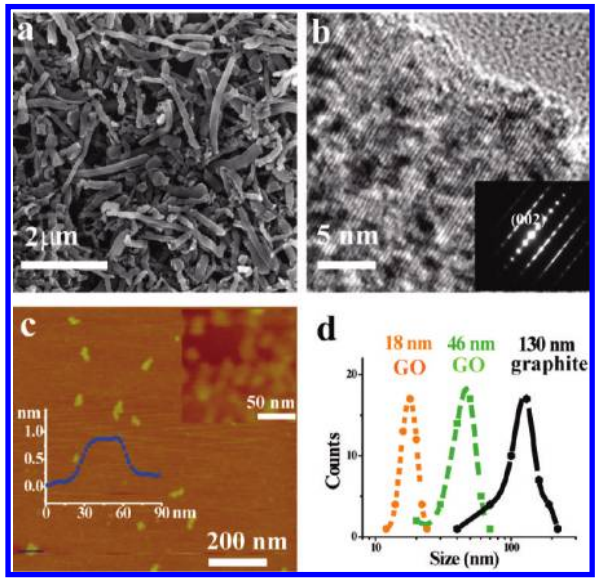

Figure 1. GO nanosheets synthesized from graphite nanofibers. (a) SEM image of the graphite nanofiber precursor. (b) HRTEM image and ED pattern (inset), showing that the graphene planes are coin-stacked along the ⟨001⟩ fiber growth direction. (c) AFM image of GO nanosheets obtained after 2 and 12 h (inset) of reaction, deposited on mica. Their apparent thickness was found to be around 1 nm, as shown in the height profile taken along the blue line. (d) Size distribution of the starting graphite nanofibers (solid black line) and GO nanosheets obtained after 2 (dashed green line) and 12 h of oxidation (dotted orange line).

The graphite nanofibers (Catalytic Materials LLC) used in this work have an average diameter of about 130 nm, with length up to a few micrometers, as shown in the scanning electron microscopy (SEM) image in Figure 1a. In the highly crystalline nanofibers, the graphene sheets are coin-stacked along the ⟨001⟩ fiber growth direction, as shown in the high-resolution transmission electron microscopy (HRTEM) and electron diffraction (ED) patterns (Figure 1b). The nanofibers were oxidized using a modified Hummer's method[2] with a preoxidation step and then purified with an acid−acetone wash procedure we recently developed.[24] In parallel, regular GO was synthesized using the same procedure from graphite powders (Bay carbon, SP-1).[24,25]

Relatively uniform GO nanosheets were obtained, with average size tunable by reaction time. Since the size upper limit is set by

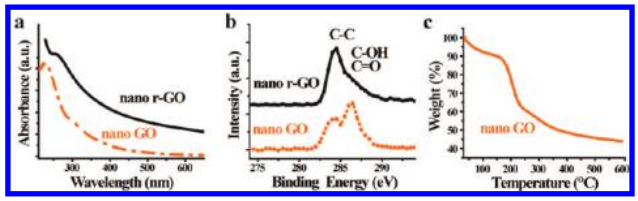

Figure 2. (a) UV/vis and (b) XPS spectra of nano GO before (brown line) and after hydrazine reduction (black line). (c) Thermogravimetric analysis curve of the nano GO, exhibiting weight loss similar to that observed with regular GO.

the diameter of the nanofibers, GO nanosheets are more uniform than regular GO. After 2 h of reaction, the average size of GO was found to be around 50 nm (Figure 1c), which decreased to ca. 20 nm after 12 h of reaction (Figure 1c, inset and d). The apparent thickness of the GO nanosheets was measured to be around 1 nm by atomic force microscopy (AFM), which is consistent with that of regular GO.[25,26] Since the diameter of the graphite nanofibers can be controlled from a few to a few hundreds of nanometers during chemical vapor deposition,[22,23] by selecting the properly sized graphite nanofibers and controlling the oxidation time, the size of GO nanosheets should be continuously tunable in this range.

The UV/vis spectrum of the nano GO dispersion (Figure 2a) shows a peak at 225 nm, slightly blue-shifted compared to that of regular GO at 230 nm, indicating a modest decrease in the size of the π conjugation domains. The nano GO can be reduced by hydrazine, after which its absorption peak was red-shifted and the overall absorption was greatly increased. This is consistent with the color change of the colloidal dispersion from brown to black, similar to what has been observed with regular GO.[27] X-ray photoelectron spectroscopy (XPS) confirmed that hydrazine reduction significantly reduced the oxygen content in the sample (Figure 2b). The nano GO can also be reduced by thermal treatment. Figure 2c shows its thermal gravimetric response upon heating in a N_2 atmosphere. A nearly 10% weight loss occurred at about 100 °C, which can be attributed to absorbed water. Another major weight loss of nearly 40% was observed between 200 and 300 °C, corresponding to the deoxygenating reactions as observed in regular GO.[28] The results in Figure 2 suggest that, in terms of spectroscopic characteristics and chemical properties, these GO nanosheets are very similar to regular micrometer-sized GO.[4,7,8]

However, size is very important for the surface activity of GO. Regular micrometer-sized GO colloids tend to migrate to the water surface over time,[15,29−31] as shown in the Brewster angle microscopy (BAM) image (Figure 3a). This eventually leads to a GO thin film covering the surface of an evaporating droplet, which leaves a continuous film after drying (Figure 3c, left and d). In contrast, the GO nanosheets preferably stay in water (Figure 3b). A droplet of GO nanocolloids tends to leave the typical "coffee ring stain" [32,33] type of drying pattern, just like common water-soluble or dispersible materials (Figure 3c, right and e). The different drying behaviors between regular and nano GO colloids were consistently observed over a wide range of concentrations from 0.01 to 1 mg/mL (Supporting Information (SI) Figure S1). Since evaporation is a fundamental step in all solution-processing techniques, the knowledge of size-dependent drying behaviors should be useful for the fabrication of GO-based thin films and coatings.

The decreased surface activity of GO nanosheets is likely due to their higher edge-to-area ratio, which increases their charge density and makes them more hydrophilic. This has been confirmed by zeta-potential measurements, as shown in Figure 4a. The higher charge density on GO nanosheets also significantly increases their colloidal stability. GO nanocolloids remained stable even after

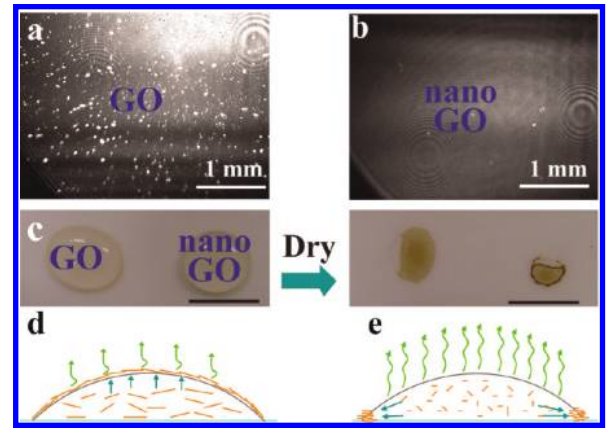

Figure 3. Surface activity of regular and nano GO. (a,b) *In situ* BAM observation of air−water interface during evaporating a GO and GO nanocolloidal solutions, respectively. Regular GO sheets tend to enrich at the water surface over time, but nano GO is much less surface active. Therefore, regular GO colloids tend to develop a coating on the water surface during evaporation and leave a continuous film after drying (c,d). In contrast, GO nanocolloids tend to leave the typical "coffee ring stain" type of drying marks commonly seen for aqueous colloidal dispersions (c,e). The scale bars in panel c represent 1 cm.

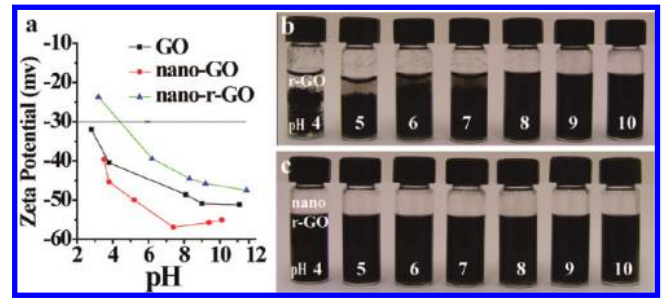

Figure 4. Enhanced colloidal stability of nano GO and nano r-GO. (a) Zeta-potential measurement of water dispersion of GO, nano GO, and nano r-GO. Values of r-GO sheets could not be measured due to heavy aggregation (b). GO nanocolloids appear to have higher charge density, which is consistent with their greatly reduced size and increased edge-to-center ratio. Therefore, they are much more stable than regular GO (see Figure S2). In contrast to regular r-GO (b), the r-GO nanocolloids (c) are also much more stable, resulting in stable colloidal dispersion over a wide range of solution pH values.

centrifugation at 10 000 rpm for 30 min, while the regular GO colloids started to precipitate at 5000 rpm (SI Figure S2). It has been well known that r-GO colloids are less stable in water due to increased $\pi-\pi$ stacking between the deoxygenated surfaces.[27] As seen in Figure 4d, hydrazine-reduced r-GO sheets indeed aggregated under most of the pH values from 4 to 10, thus preventing zeta-potential measurements. However, r-GO nanosheets were found to be stable in the entire range of pH values (Figure 4c). With GO or r-GO sheets, their colloidal stability is determined by the competition between repulsive electrostatic interaction and attractive, face-to-face van der Waals interaction of overlapping sheets.[25,34] The enhanced colloidal stability of nano GO and r-GO is attributed to a combination of increased electrostatic repulsion, reduced overlapping areas, and reduced probability of overlapping due to smaller areas of the nanosheets.

The enhanced colloidal stability of GO nanosheets should make them excellent dispersing agents for processing insoluble materials. In an earlier report, we showed that GO can act as a surfactant to disperse graphite powders and carbon nanotubes in water.[31] Here, the performances of regular GO and nano GO as dispersing agents for unfunctionalized single-walled nanotubes (SWCNTs) (Carbon

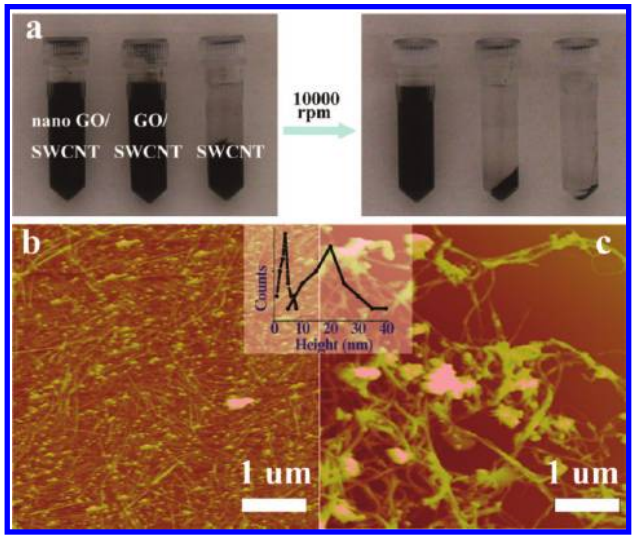

Figure 5. Nano GO as a dispersing agent. (a) Both GO and nano GO can disperse unfunctionalized SWCNTs in water after sonication, but the resulting colloidal dispersion using nano GO is much more stable, as seen in the centrifugation test. (b,c) AFM images show that the SWCNTs were disentangled and debundled after being sonicated in nano GO dispersion. The average height of SWCNTs decreases from ~20 nm in water to ~4 nm after dispersion (inset).

Solutions, Inc., P2-SWNT) were compared. Figure 5a shows the dispersions of 1 mg of SWCNTs after being sonicated for 2 h in 2 mL of nano GO, regular GO (both 1 mg/mL), and deionized water, respectively. The SWCNTs precipitated right after sonication. Both of the GO samples were able to disperse the nanotubes. However, the dispersion created using nano GO as surfactant was significantly more stable, as shown by the centrifugation test. The UV/vis spectrum (SI Figure S3) of the nano GO/SWCNTs dispersion shows the characteristic peaks of SWCNTs at 750 nm and nano GO at 230 nm, both red-shifted, suggesting a strong $\pi-\pi$ interaction between them. The AFM image of the starting SWCNTs show that the tubes were heavily entangled and bundled. The average bundle diameter measured by the height profile was ~20 nm (Figure 5c). In contrast, nano GO dispersed SWCNTs were largely disentangled and debundled, with average diameter reduced to ~4 nm (Figure 5b). AFM studies found that the nanotubes are only partially covered by GO nanosheets (SI Figure S4). Therefore, the nano GO/SWCNT complex is still conductive, and the conductivity can be further increased by reducing the nano GO after solution processing (SI Figure S5).

In summary, uniform GO nanocolloids can be directly synthesized using crystalline graphite nanofibers as the starting material. The diameter of the nano GO is determined by the nanofiber diameter and the oxidation time. GO nanosheets were found to be more hydrophilic than their regular, micrometer-sized counterparts, resulting in very different drying behaviors. The small size of nano GO also greatly enhances their colloidal stability. Even nano r-GO sheets are stable in a wide range of pH values. The enhanced stability of GO nanocolloids should make them very promising dispersing agents for insoluble, aromatic materials such as SWCNTs.

Acknowledgment. This work was primarily supported by the National Science Foundation (CAREER DMR 0955612). Additional support was provided by the Initiative for Sustainability and Energy at Northwestern (ISEN) (V.C.T, A.T.L.T., and P.E.G.), a seed grant from the Northwestern Nanoscale Science and Engineering Center (NSF EEC 0647560) (J.L), and the Sony Corp. L.J.C. is a NSF graduate research fellow. A.T.L.T. thanks the Defence Science and Technology Agency of Singapore for an overseas undergraduate scholarship. We thank the Northwestern Materials Research Science and Engineering Center (NSF DMR-0520513) for a capital equipment fund for the purchase of BAM. Microscopy and surface analysis were carried out at the NU*ANCE* center at Northwestern University.

Supporting Information Available: Experimental details and other supplementary data. This materials is available free of charge via Internet at http://pubs.acs.org.

References

(1) Brodie, B. C. *Philos. Trans. R. Soc. London* **1859**, *149*, 249–259.
(2) Hummers, W. S.; Offeman, R. E. *J. Am. Chem. Soc.* **1958**, *80*, 1339–1339.
(3) Li, D.; Kaner, R. B. *Science* **2008**, *320*, 1170–1171.
(4) Park, S.; Ruoff, R. S. *Nature Nanotechnol.* **2009**, *4*, 217–224.
(5) Lerf, A.; He, H. Y.; Forster, M.; Klinowski, J. *J. Phys. Chem. B* **1998**, *102*, 4477–4482.
(6) Erickson, K.; Erni, R.; Lee, Z.; Alem, N.; Gannett, W.; Zettl, A. *Adv. Mater.* **2010**, *22*, 4467–4472.
(7) Allen, M. J.; Tung, V. C.; Kaner, R. B. *Chem. Rev.* **2009**, *110*, 132–145.
(8) Compton, O. C.; Nguyen, S. T. *Small* **2010**, *6*, 711–723.
(9) Zhang, L.; Liang, J. J.; Huang, Y.; Ma, Y. F.; Wang, Y.; Chen, Y. S. *Carbon* **2009**, *47*, 3365–3368.
(10) Luo, Z. T.; Lu, Y.; Somers, L. A.; Johnson, A. T. C. *J. Am. Chem. Soc.* **2009**, *131*, 898–899.
(11) Son, Y. W.; Cohen, M. L.; Louie, S. G. *Nature* **2006**, *444*, 347–349.
(12) Jiao, L. Y.; Zhang, L.; Wang, X. R.; Diankov, G.; Dai, H. J. *Nature* **2009**, *458*, 877–880.
(13) Kosynkin, D. V.; Higginbotham, A. L.; Sinitskii, A.; Lomeda, J. R.; Dimiev, A.; Price, B. K.; Tour, J. M. *Nature* **2009**, *458*, 872–876.
(14) Cai, J. M.; Ruffieux, P.; Jaafar, R.; Bieri, M.; Braun, T.; Blankenburg, S.; Muoth, M.; Seitsonen, A. P.; Saleh, M.; Feng, X. L.; Mullen, K.; Fasel, R. *Nature* **2010**, *466*, 470–473.
(15) Kim, J.; Cote, L. J.; Kim, F.; Yuan, W.; Shull, K. R.; Huang, J. *J. Am. Chem. Soc.* **2010**, *132*, 8180–8186.
(16) Sun, X. M.; Liu, Z.; Welsher, K.; Robinson, J. T.; Goodwin, A.; Zaric, S.; Dai, H. J. *Nano Res.* **2008**, *1*, 203–212.
(17) Liu, Z.; Robinson, J. T.; Sun, X.; Dai, H. *J. Am. Chem. Soc.* **2008**, *130*, 10876–10877.
(18) Yang, X.; Zhang, X.; Liu, Z.; Ma, Y.; Huang, Y.; Chen, Y. *J. Phys. Chem. C* **2008**, *112*, 17554–17558.
(19) Zhang, L.; Xia, J.; Zhao, Q.; Liu, L.; Zhang, Z. *Small* **2010**, *6*, 537–544.
(20) Sun, X. M.; Luo, D. C.; Liu, J. F.; Evans, D. G. *ACS Nano* **2010**, *4*, 3381–3389.
(21) Green, A. A.; Hersam, M. C. *J. Phys. Chem. Lett.* **2010**, *1*, 544–549.
(22) Rodriguez, N. M. *J. Mater. Res.* **1993**, *8*, 3233–3250.
(23) Rodriguez, N. M.; Chambers, A.; Baker, R. T. K. *Langmuir* **1995**, *11*, 3862–3866.
(24) Kim, F.; Luo, J.; Cruz-Silva, R.; Cote, L. C.; Sohn, K.; Huang, J. *Adv. Funct. Mater.* **2010**, *20*, 2867–2873.
(25) Cote, L. J.; Kim, F.; Huang, J. *J. Am. Chem. Soc.* **2009**, *131*, 1043–1049.
(26) Stankovich, S.; Dikin, D. A.; Piner, R. D.; Kohlhaas, K. A.; Kleinhammes, A.; Jia, Y.; Wu, Y.; Nguyen, S. T.; Ruoff, R. S. *Carbon* **2007**, *45*, 1558–1565.
(27) Li, D.; Muller, M. B.; Gilje, S.; Kaner, R. B.; Wallace, G. G. *Nature Nanotechnol.* **2008**, *3*, 101–105.
(28) Becerril, H. c. A.; Mao, J.; Liu, Z.; Stoltenberg, R. M.; Bao, Z.; Chen, Y. *ACS Nano* **2008**, *2*, 463–470.
(29) Chen, C.; Yang, Q.-H.; Yang, Y.; Lv, W.; Wen, Y.; Hou, P.-X.; Wang, M.; Cheng, H.-M. *Adv. Mater.* **2009**, *21*, 3007–3011.
(30) Zhu, Y.; Cai, W.; Piner, R. D.; Velamakanni, A.; Ruoff, R. S. *Appl. Phys. Lett.* **2009**, *95*, 103104.
(31) Kim, F.; Cote, L. J.; Huang, J. *Adv. Mater.* **2010**, *22*, 1954–1958.
(32) Deegan, R. D.; Bakajin, O.; Dupont, T. F.; Huber, G.; Nagel, S. R.; Witten, T. A. *Nature* **1997**, *389*, 827–829.
(33) Deegan, R. D. *Phys. Rev. E* **2000**, *61*, 475–485.
(34) Israelachvili, J. N. *Intermolecular and Surface Forces*, 2nd ed.; Academic Press: San Diego, 1992.

JA1078943